

# Cobalt and Molybdate Ions Effects on the Passivation of Iron Based FeCoC Ternary Alloys, in non Deaerated Solution of $10^{-3}$ M NaHCO<sub>3</sub> + $10^{-3}$ M Na<sub>2</sub>SO<sub>4</sub>, at 25 °C

F. Haddad,\* A. Benchettara, S.E. Amara, R. Kesri

*Laboratoire d'Electrochimie-Corrosion, Métallurgie et Chimie Minérale, Faculté de Chimie, U. S. T. H. B., B. P. 32, El Alia, Bab Ezzouar (16111), Alger, Algérie*

Received 25 April 2007; accepted 4 July 2007

---

## Abstract

In the present paper, the electrochemical behaviour of four based iron FeCoC ternary alloys was studied in non deaerated solution of  $10^{-3}$  M NaHCO<sub>3</sub> +  $10^{-3}$  M Na<sub>2</sub>SO<sub>4</sub>, at 25 °C, and compared to that of pure iron and cobalt. The inhibition effect of sodium molybdate has also been considered for different concentrations. It was noted that the oxygen oxidizes the FeCoC ternary alloys except that with the most important cobalt content.

For this reason, a potentiodynamic polarisation was carried out at different temperatures (25, 35, 45 and 55°C) in which the current growth versus temperature indicates really that molybdate oxidizes this alloy.

**Keywords:** iron, cobalt, FeCoC ternary alloys, bicarbonate, sodium molybdate.

---

## Introduction

This work constitutes the continuation of a study that we carry out actually concerning the plot of the liquidus projection of the Fe-Co-C system in the iron rich corner.

In this part of the work, the potentiodynamic technique was applied to compare the electrochemical behaviour of iron, cobalt and based iron FeCoC ternary alloys in non deaerated solution. This latter contained  $10^{-3}$  M NaHCO<sub>3</sub> and  $10^{-3}$  M Na<sub>2</sub>SO<sub>4</sub>.

---

\* Corresponding author. E-mail address: hf76dz@hotmail.com

The inhibition effect of sodium molybdate was also studied for different concentrations (0 M,  $10^{-4}$  M,  $10^{-3}$  M and  $10^{-2}$  M) at 25 °C. Temperature effect was studied for one FeCoC ternary alloy in the range of 25 to 55 °C with a variation step of 10 °C. Sodium molybdate inhibitors are becoming more and more attractive in an increasing number of applications because of their low order of toxicity and environment compatibility. Sodium molybdate is widely used for example as corrosion inhibitor in cooling tower water [1-3] and for boiler feed water systems [4]. Its popularity stems from its ability to inhibit both the general and the pitting corrosion of ferrous [5-13] and nonferrous metals [14-17] and its effectiveness in waters ranging from zero to high hardness, low conductivity to high salinity, and pH from 5 to above 10 [18]. However, molybdate, being a much weaker oxidizing agent, could not passivate in the absence of oxygen [6, 19-21]. It was suggested that in aerated environment, oxygen was the primary passivator, and the inhibiting anions acted only in film repair [7].

### Experimental procedure

First, the alloys were arc melted in an argon gas atmosphere from pure metals and graphite. Their compositions are listed in table 1.

**Table 1:** Compositions of the FeCoC studied alloys.

Alloys	Compositions /weight % (wt. %)		
	Co	C	Fe
Co2b	4.84	4.20	90.96
Co2a	6.50	4.13	89.37
Co5a	7.25	0.50	92.25
Co5b	10.00	0.48	89.52

The electrochemical tests were conducted using a VoltaLAB PGZ301 potentiostat. The potential of the working electrode was measured against a saturated calomel reference electrode (SCE). The auxiliary electrode was platinum (Pt). The working electrode surfaces were mechanically ground with emery paper (400 to 1200), polished with alumina (1  $\mu$ m and 200 Å) and rinsed with distilled water. The corrosive medium consisted of neutral aqueous solution  $10^{-3}$  M  $\text{Na}_2\text{SO}_4$  and  $10^{-3}$  M  $\text{NaHCO}_3$ . Several concentrations (ranging from  $10^{-4}$  M to  $10^{-2}$  M) of sodium molybdate, in the form of  $\text{Na}_2\text{MoO}_4 \cdot 2\text{H}_2\text{O}$  (Fluka), were added to the test solution as corrosion inhibitors.

The polarisation curves are plotted in potentiodynamic mode. Before each polarisation, the working electrodes were immersed in the test solution for 45 min. Then, the electrode potential was scanned from -0.8 V/SCE to +1 V/SCE in the direction of the increasing potentials at a scanning rate of  $1 \text{ mV} \cdot \text{s}^{-1}$ . This rate is sufficiently slow to allow a stationary state setting at each point of the curve. The electrochemical experiments were carried out at 25 °C with agitation in presence of oxygen.

### Results and discussion

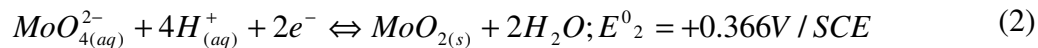
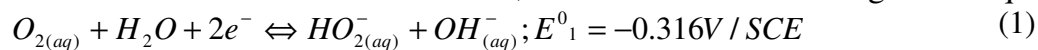
In absence of sodium molybdate, Co5b ternary alloy, with the most important cobalt content, has a corrosion current density lower than that of iron ( $i_{cor} = 1.7 \mu\text{A cm}^{-2}$  for a corrosion potential of  $-0.337 \text{ V/SCE}$ ) in  $10^{-3} \text{ M NaHCO}_3 + 10^{-3} \text{ M Na}_2\text{SO}_4$  aqueous solution at  $25^\circ \text{C}$ . For comparison, pure iron is characterized by a corrosion potential of  $-0.343 \text{ V/SCE}$  and a corrosion current density of  $3.3 \mu\text{A cm}^{-2}$  in the same conditions.

**Table 2.**  $E_{cor}$  in V/ECS and  $i_{cor}$  in  $\mu\text{A cm}^{-2}$  of iron, cobalt and FeCoC ternary alloys, immersed in  $10^{-3} \text{ M NaHCO}_3 + 10^{-3} \text{ M Na}_2\text{SO}_4$ , at  $25^\circ \text{C}$ , in absence and in presence of different concentrations of  $\text{MoO}_4^{2-}$ .

[ $\text{MoO}_4^{2-}$ ]	Fe		Co		Co5b		Co5a		Co2a		Co2b	
	$E_{cor}$	$i_{cor}$										
0 M	-343	3.3	-406	2.9	-337	1.7	-347	1.8	-390	18.2	-395	16.8
$10^{-4} \text{ M}$	-532	6.4	-403	5.1	-328	2.7	-318	1.6	-441	3.6	-415	15.2
$10^{-3} \text{ M}$	-459	8.5	-393	3.6	-359	6.1	-357	7.8	-384	7.0	-386	9.0
$10^{-2} \text{ M}$	-449	12.0	-446	8.6	-562	12.9	-330	2.6	-337	2.7	-382	3.8

If sodium molybdate accelerates the corrosion rate of Co5b ternary alloy in the range of concentration  $10^{-4} - 10^{-2} \text{ M}$ , it confers to this alloy, however, a quasi-passive state for a concentration of  $10^{-2} \text{ M}$  (table 2). In presence of  $10^{-2} \text{ M MoO}_4^{2-}$ , the corrosion current densities of Co5a, Co2a and Co2b are lower than that of iron.

Dissolved oxygen and molybdate ion, oxidized forms in the redox couples  $\text{O}_{2(aq)} / \text{HO}_{2(aq)}^-$  and  $\text{MoO}_{4(aq)}^{2-} / \text{MoO}_{2(s)}$ , can be reduced according to the equations:



At  $\text{pH} = 7.9$ , the equilibrium potential of redox couple  $\text{O}_{2(aq)} / \text{HO}_{2(aq)}^-$ , calculated from equation (1) at  $25^\circ \text{C}$ , is  $E_{eq1} = -0.136 \text{ V/SCE}$ , whereas the equilibrium potentials of  $\text{MoO}_{4(aq)}^{2-} / \text{MoO}_{2(s)}$ , calculated by application of Nernst relation to equation (2), are  $E_{eq1a} = -0.685$ ,  $E_{eq1b} = -0.656$  and  $E_{eq1c} = -0.626 \text{ V/ECS}$  at, respectively,  $10^{-4} \text{ M}$ ,  $10^{-3} \text{ M}$  and  $10^{-2} \text{ M}$  in sodium molybdate.

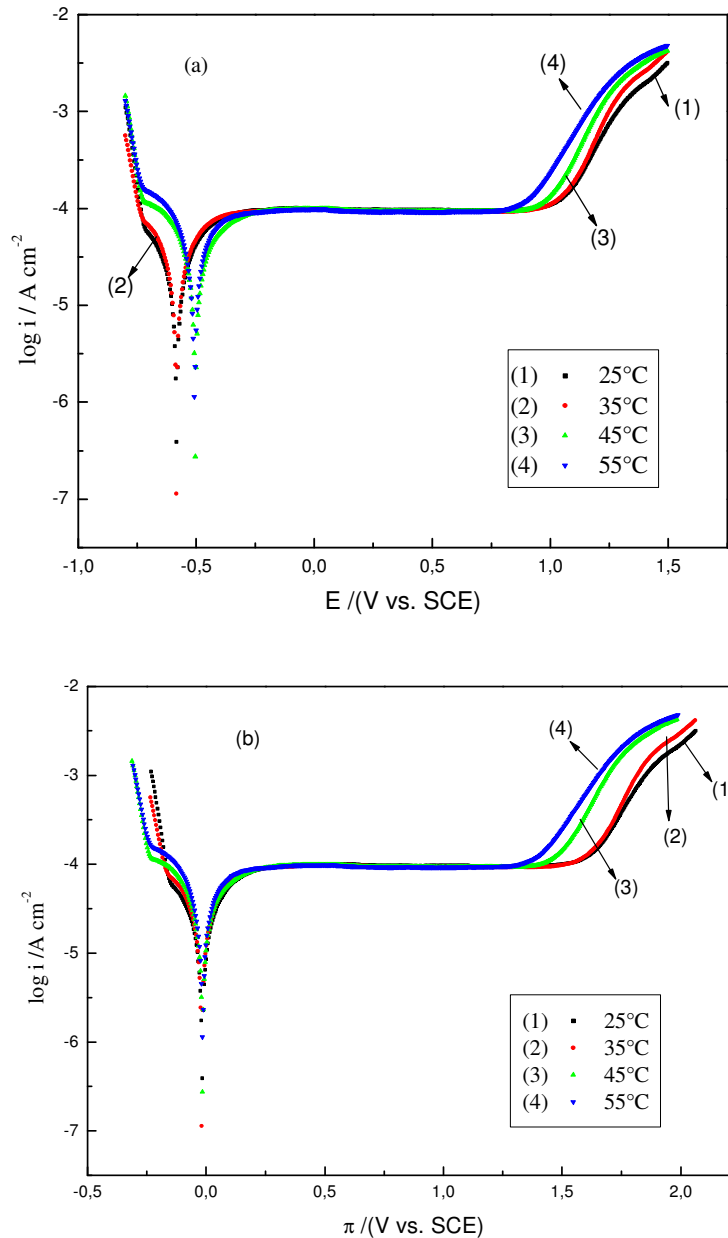


**Figure 1.** Potentiodynamic polarisation curves of Co5b in non deaerated solution of  $10^{-3}$  M  $\text{NaHCO}_3$  and  $10^{-3}$  M  $\text{Na}_2\text{SO}_4$  at  $10^{-2}$  M sodium molybdate, at 25, 35, 45 and 55 °C (a)  $\log i = f(E)$ , (b)  $\log i = f(\pi)$ .

Table 2 shows that, aside from the Co5b corrosion potential in presence of  $10^{-2}$  M sodium molybdate, which is close to  $E_{\text{eq}1c}$ , all other potentials are more positive than  $E_{\text{eq}1a}$ ,  $E_{\text{eq}1b}$  and  $E_{\text{eq}1c}$ . For this reason, excepting Co5b, whose corrosion can be thermodynamically caused by  $10^{-2}$  M  $\text{MoO}_4^{2-}$ , the molybdate ion can't oxidize neither iron nor FeCoC ternary alloys. On the other hand, all corrosion potentials given in table 1 are more cathodic than equilibrium potential of dioxygen,  $E_{\text{eq}1}$ . This last observation enables us to affirm that the corrosive agent of iron and the three ternary alloys Co5a, Co2a and Co2b in  $10^{-3}$  M

$\text{NaHCO}_3 + 10^{-3} \text{ M Na}_2\text{SO}_4 + x \text{ M Na}_2\text{MoO}_4$ , with ( $x = 0-10^{-2}$ ), is the dissolved dioxygen.

The assumption that  $10^{-2} \text{ M}$  sodium molybdate oxidizes the Co5b ternary alloy is confirmed by the study of temperature effect between 25 and 55 °C at this concentration. The polarisation curves (Fig. 1) show that the reduction current rises with the temperature augmentation, confirming that molybdate oxidizes effectively this alloy. In fact, if oxygen would oxidize the alloy, one could observe diffusion plateaux which decreases with the temperature increase, taking into account the diminution of oxygen solubility in corrosive medium when the temperature rises. Fig. 2 shows the linear variation of  $\log i_{\text{cor}}$  versus  $1000/T$ .

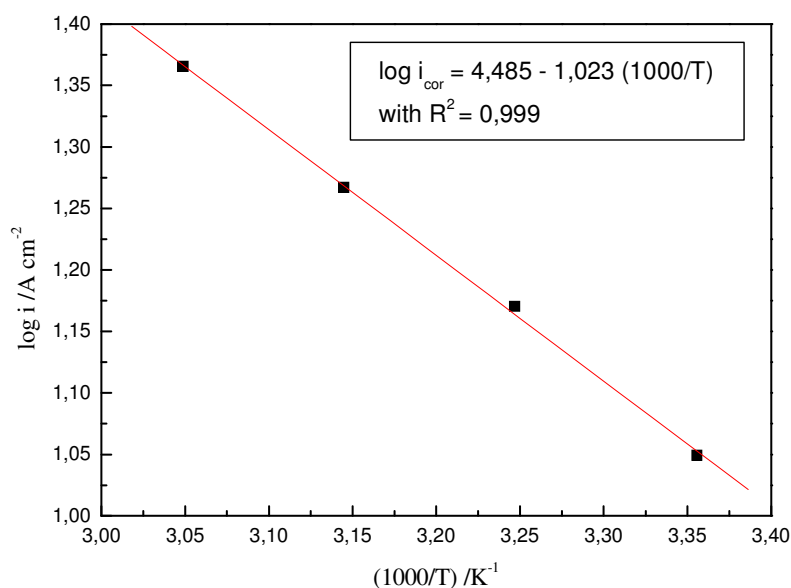


**Figure 2.** Variation of  $\log i_{\text{cor}}$  versus  $1000/T$  for Co5b ternary alloy.

### Cathodic reduction on iron

Fig. 3a shows that iron corrosion potential in  $10^{-3} \text{ M NaHCO}_3 + 10^{-3} \text{ M Na}_2\text{SO}_4 + x \text{ M Na}_2\text{MoO}_4$ , with ( $x = 10^{-4} - 10^{-2}$ ) shifts towards more cathodic values than in absence of molybdate. Fig. 3b reveals that molybdate ion modifies the kinetic of the cathodic reduction process on the interface Fe /  $10^{-3} \text{ M NaHCO}_3 + 10^{-3} \text{ M Na}_2\text{SO}_4 + x' \text{ M Na}_2\text{MoO}_4$ ,  $x' = 0-10^{-2} \text{ M}$ . In fact, in absence of sodium molybdate, the cathodic curve form of Fig. 3 shows that the dioxygen reduction is governed by an activation-diffusion mixed kinetic. When sodium molybdate is added to corrosive medium, it improves the electric conductivity of this medium and consequently accelerates the charge transfer step of the cathodic process and makes of the diffusion of dioxygen towards the interface metal/solution the determining step. Thus, the cathodic process which was under mixed control of activation-diffusion, in absence of molybdate, passes under diffusion control when sodium molybdate is added to corrosive solution.

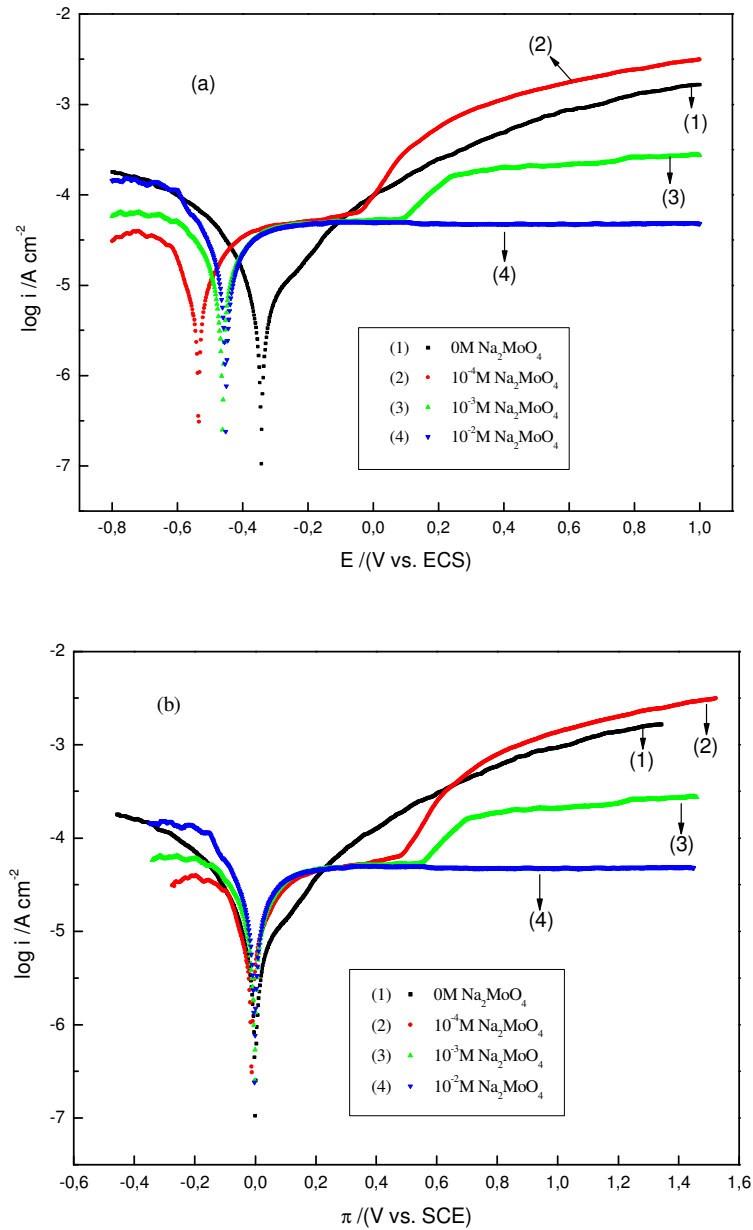


**Figure 3.** Potentiodynamic polarisation curves of pure iron in non deaerated solution of  $10^{-3}$  M  $\text{NaHCO}_3$  and  $10^{-3}$  M  $\text{Na}_2\text{SO}_4$  in absence and in presence of sodium molybdate, at 25 °C. (a)  $\log i = f(E)$ , (b)  $\log i = f(\pi)$ .

It can be observed in table 2 that the increase of sodium molybdate concentration, between  $10^{-4}$  and  $10^{-2}$  M, leads to increase the current density and to displace the corrosion potential towards more anodic values. Molybdate ions being thermodynamically non reducible, in this work conditions, the increase of current density with anodic displacement of corrosion potential can be interpreted by a kinetic character of reduction process of dioxygen in presence of molybdate ions.

The limit diffusion current density  $i_d$  is related to the dissolved oxygen concentration by the relation

$$i_d = k(O_2) \quad (3)$$

where  $k$  is the kinetic constant of mass transfer on the interface Fe /  $10^{-3}$  M NaHCO<sub>3</sub> +  $10^{-3}$  M Na<sub>2</sub>SO<sub>4</sub> +  $x$  M Na<sub>2</sub>MoO<sub>4</sub>, with  $x = 10^{-4}$ - $10^{-2}$  M.

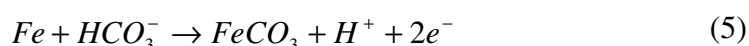
**Table 3.** Diffusion current density  $i_d$  of dioxygen and kinetic constant  $k$  versus sodium molybdate concentration, at 25 °C.

(MoO <sub>4</sub> <sup>2-</sup> ) / M	(O <sub>2</sub> ) / M	10 <sup>+5</sup> . $i_d$ / $\mu$ A cm <sup>-2</sup>	10 <sup>+5</sup> . $k$ / A cm mol <sup>-1</sup>
10 <sup>-4</sup>	1.27 10 <sup>-3</sup> [22]	7.94	6.25
10 <sup>-3</sup>		8.91	7.02
10 <sup>-2</sup>		10.6	8.34

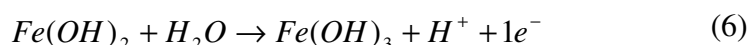
When table 3 is examined, it is seen that the constant  $k$  value, calculated from equation (3), increases with the increase of MoO<sub>4</sub><sup>2-</sup> concentration, for a constant concentration of dioxygen, at 25 °C. This observation offers the possibility to apply this result to the electrochemical dosage of molybdate ion on iron electrode.

### Anodic oxidation of iron

Fig. 3b shows that in absence of sodium molybdate, iron is oxidized actively along the anodic polarisation. The inflection point of the anodic curve at approximately +0.10 V/SCE, informs about a change in oxidation degree of corrosion products. In fact, below the inflection point, the active dissolution of iron [23] leads to the formation of iron (II) hydroxide and iron (II) carbonate, according to the equations

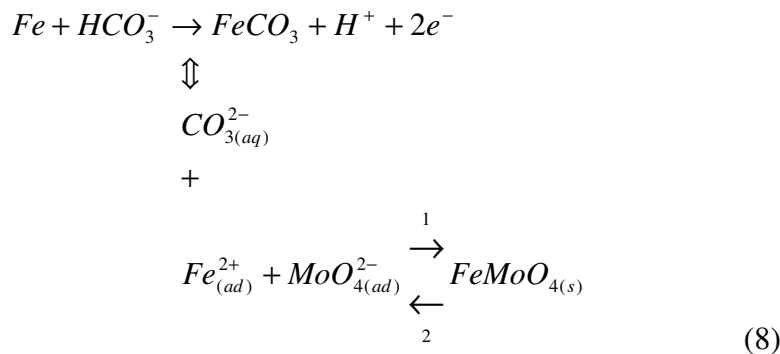
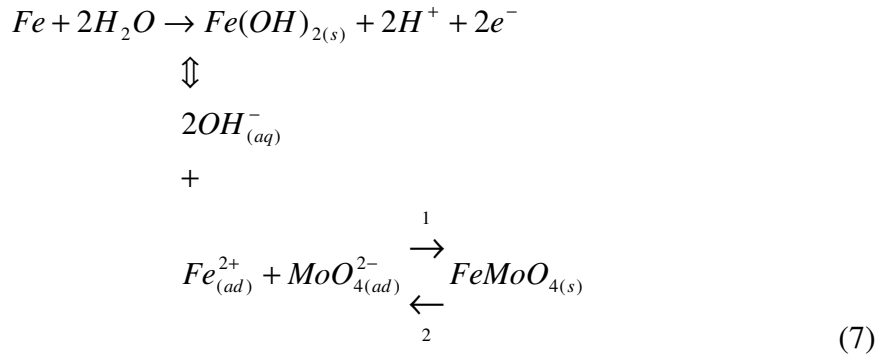


Beyond the inflection point, the corrosion products are oxidized in a higher oxidation state:



In presence of MoO<sub>4</sub><sup>2-</sup>, the active dissolution process is accelerated, nearby the corrosion potential; a quasi-passive plateau, probably due to the formation of a passive film, and whose extent augments with the increase of sodium molybdate concentration, appears at the same potential as that of the inflection point observed in absence of molybdate. In presence of 10<sup>-2</sup> M molybdate, iron reaches a quasi-passive state extending on more than 1.2 V, with a passive current density of 90  $\mu$ A.cm<sup>-2</sup>. Inhibition by molybdate ions involves its incorporation in the film, probably in a reduced form [6, 21, 24-27].

For concentrations of  $10^{-3}$  M and  $10^{-4}$  M in sodium molybdate, the inflection point displaces towards more anodic potentials when the  $\text{MoO}_4^{2-}$  concentration is higher. At these two concentrations, the passive film doesn't cover the total iron surface since, beyond the inflection point, reaction (6) continues to occur but at decreasing rates with the raising of molybdate ion concentration. This passive film could be formed according to the following mechanism:



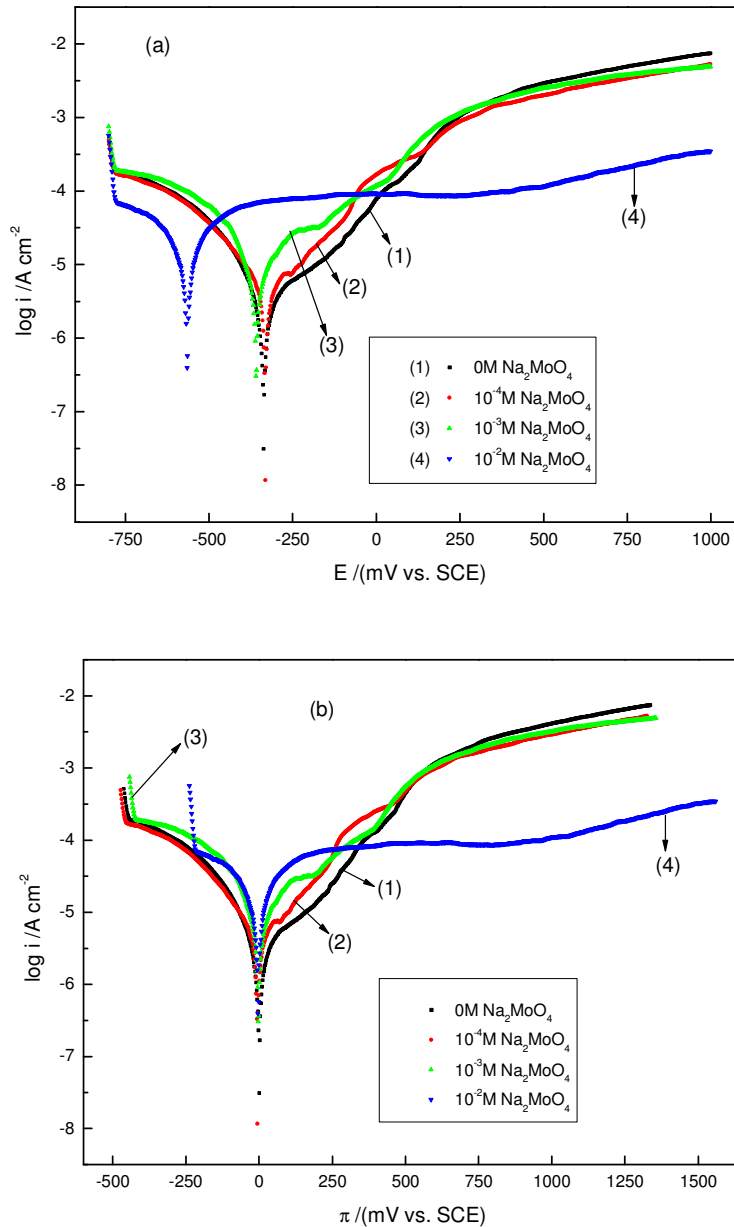
### Co5b ternary alloy

Fig. 4 gives the potentiodynamic polarisation curves of the Co5b ternary alloy immersed in non deaerated solution of  $10^{-3}$  M  $\text{NaHCO}_3$  +  $10^{-3}$  M  $\text{Na}_2\text{SO}_4$  + x M  $\text{Na}_2\text{MoO}_4$ , with  $x = 0 - 10^{-2}$  M, at  $25^\circ$  C. The cathodic curves have the same shape and are almost superposable. The presence of molybdate ions does not modify therefore the reduction kinetic of dioxygen reduction, as it is the case on iron, under the same conditions. On the other hand, the anodic curves evolve with the augmentation of sodium molybdate concentration. At concentrations of  $10^{-3}$  and  $10^{-4}$  M in sodium molybdate, the anodic curves have the same shape that in absence of  $\text{MoO}_4^{2-}$ : under these conditions, the Co5b ternary alloy undergoes an active dissolution, in the entire anodic polarisation interval; the anodic curves are characterised by two inflection points. In presence of  $10^{-2}$  M  $\text{Na}_2\text{MoO}_4$ , the curve form is different from the previous ones; it is characterised by an important cathodic shift of corrosion potential and a quasi-passive state with a current density of about  $100 \mu\text{A cm}^{-2}$ .

Beyond 0.8 V/SCE, the quasi passive plateau is stretched slightly to the top, probably indicating a reaction of anodic oxidation in solid phase.

### Co5a ternary alloy

The cathodic curves of this alloy have the same shape (Fig. 5) and are almost perfectly superposable, indicating therefore that the presence of sodium molybdate in the concentration range of  $10^{-4}$  –  $10^{-2}$  M of sodium molybdate has no effect on the cathodic process mechanism. For a concentration of  $10^{-2}$  M, the anodic process is characterised by a quasi-passive state with a passive current density of  $13.0 \mu\text{A cm}^{-2}$ .



**Figure 4.** Potentiodynamic polarisation curves of Co5b in non deaerated solution of  $10^{-3}$  M  $\text{NaHCO}_3$  and  $10^{-3}$  M  $\text{Na}_2\text{SO}_4$  in absence and in presence of sodium molybdate, at 25 °C. (a)  $\log i = f(E)$ , (b)  $\log i = f(\pi)$ .

### Co2a ternary alloy

The cathodic curves (Fig. 6) show that the dioxygen reduction process is slower in presence of  $10^{-4}$  M  $\text{MoO}_4^{-2}$  than in its absence, attesting thus the adsorption of molybdate ions on the cathodic sites of Co2a ternary alloy. At concentrations of  $10^{-3}$

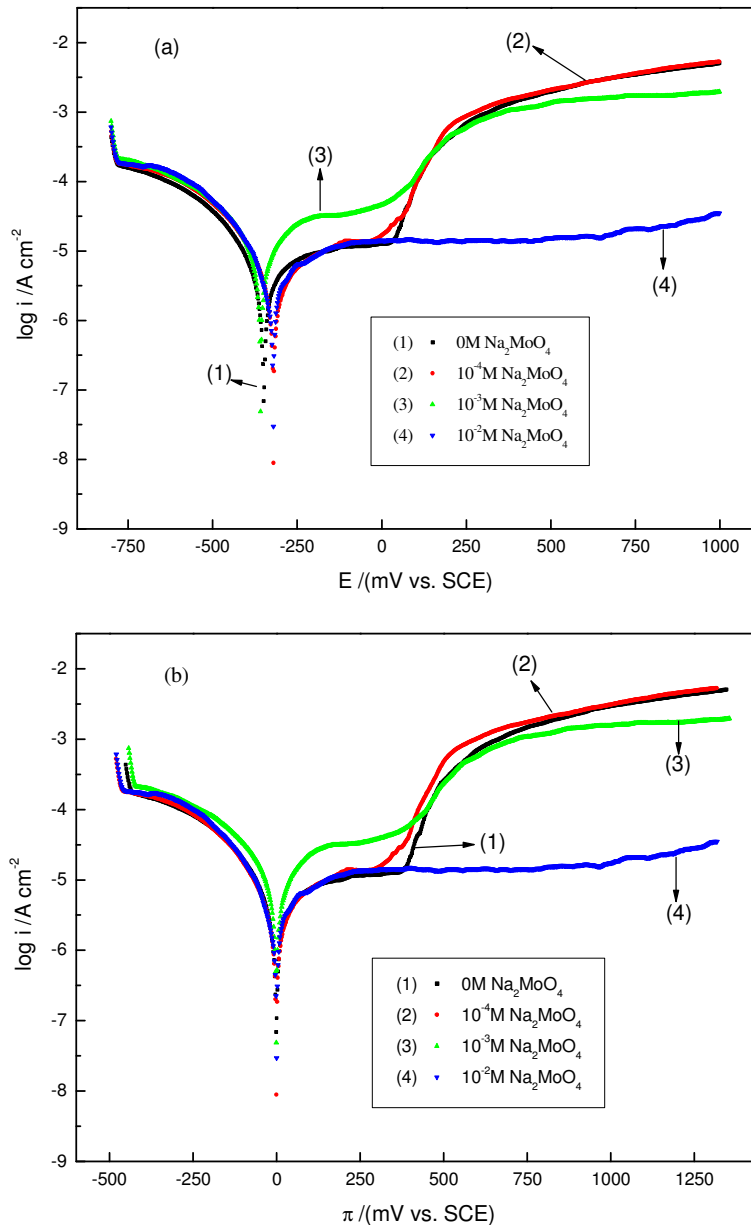


**Figure 5.** Potentiodynamic polarisation curves of Co5a in non deaerated solution of  $10^{-3}$  M  $\text{NaHCO}_3$  and  $10^{-3}$  M  $\text{Na}_2\text{SO}_4$  in absence and in presence of sodium molybdate, at 25 °C. (a)  $\log i = f(E)$ , (b)  $\log i = f(\pi)$ .

M and  $10^{-2}$  M, the increase of the corrosive medium electric conductivity compensates the decrease of reduction rate caused by molybdate adsorption, which makes tending the curves towards the same current density, for more cathodic potentials. In presence of  $10^{-2}$  M  $\text{MoO}_4^{-2}$ , the anodic shift of corrosion potential is of about 0.053 V. The anodic currents decrease progressively with

the increase of the sodium molybdate concentration and finish by tend towards a passive plateau with current density of  $20 \mu\text{A cm}^{-2}$  for concentration of  $10^{-2}$  M.

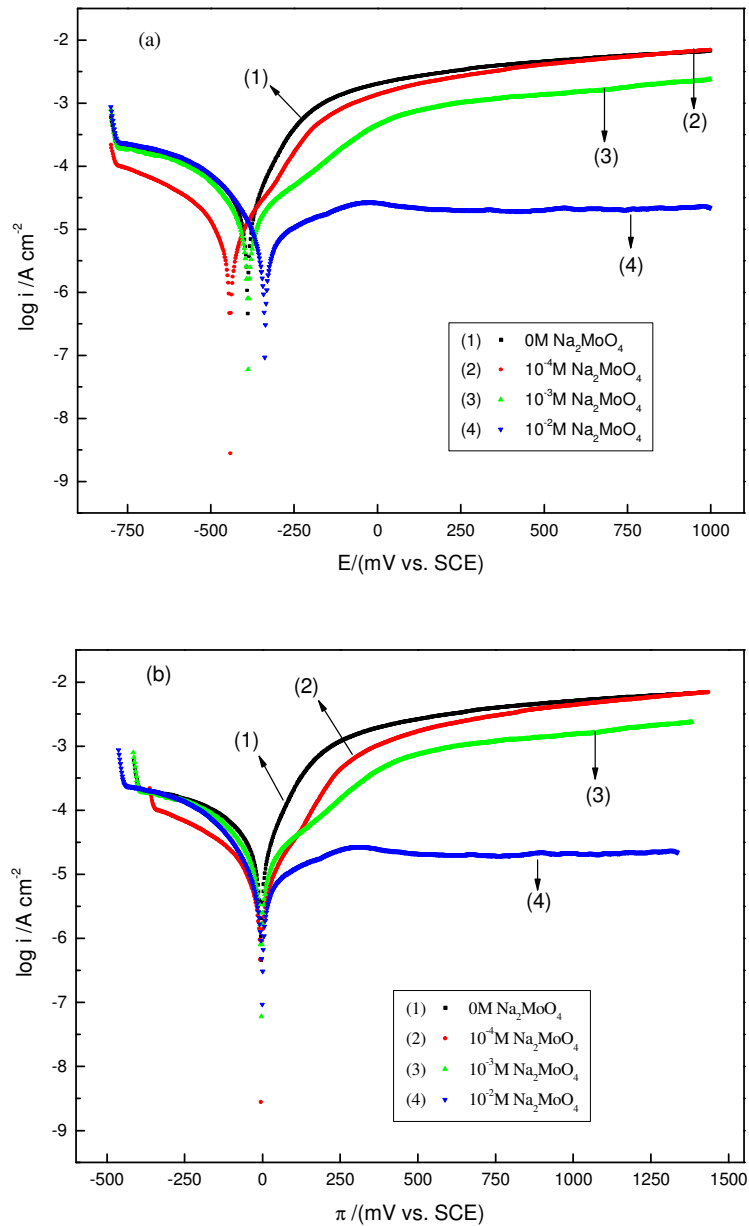


**Figure 6.** Potentiodynamic polarisation curves of Co2a in non deaerated solution of  $10^{-3}$  M  $\text{NaHCO}_3$  and  $10^{-3}$  M  $\text{Na}_2\text{SO}_4$  in absence and in presence of sodium molybdate, at  $25^\circ\text{C}$ . (a)  $\log i = f(E)$ , (b)  $\log i = f(\pi)$ .

### Co2b ternary alloy

Sodium molybdate, at the concentrations of  $10^{-4}$  and  $10^{-3}$  M, don't modify the reduction kinetic of cathodic process, whereas this process is slowed down for a concentration of  $10^{-2}$  M in sodium molybdate.

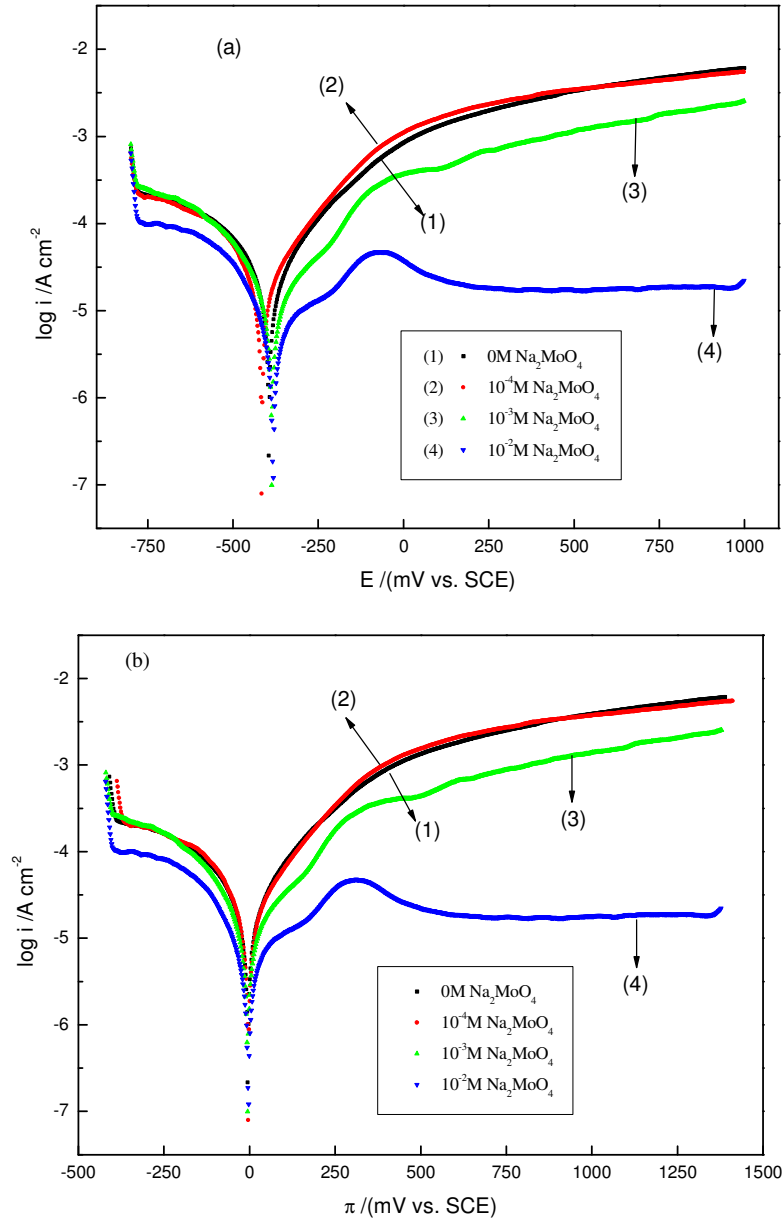


**Figure 7.** Potentiodynamic polarisation curves of Co2b in non deaerated solution of  $10^{-3}$  M  $\text{NaHCO}_3$  and  $10^{-3}$  M  $\text{Na}_2\text{SO}_4$  in absence and in presence of sodium molybdate, at 25 °C. (a)  $\log i = f(E)$ , (b)  $\log i = f(\pi)$ .

The anodic curves (Fig. 7) follow the same evolution as that on Co2a ternary alloy, except that the active-passive peak, which is hardly seen on Co2a, is well visible on Co2b ( $E_p = -0.060$  V,  $i_p = 56 \mu\text{A cm}^{-2}$ ). In presence of  $10^{-2}$  M sodium molybdate, the passivation plateau extends up to 1.3 V/SCE, with passive current density of  $20 \mu\text{A cm}^{-2}$ .

### Cobalt

With regard to Fig. 8, the addition of molybdate ions to corrosive medium does not modify the kinetic of dioxygen cathodic reduction. The rise of molybdate

concentration has however slightly accelerated the reduction rate, in particular, in presence of  $10^{-2}$  M  $\text{MoO}_4^{2-}$ .

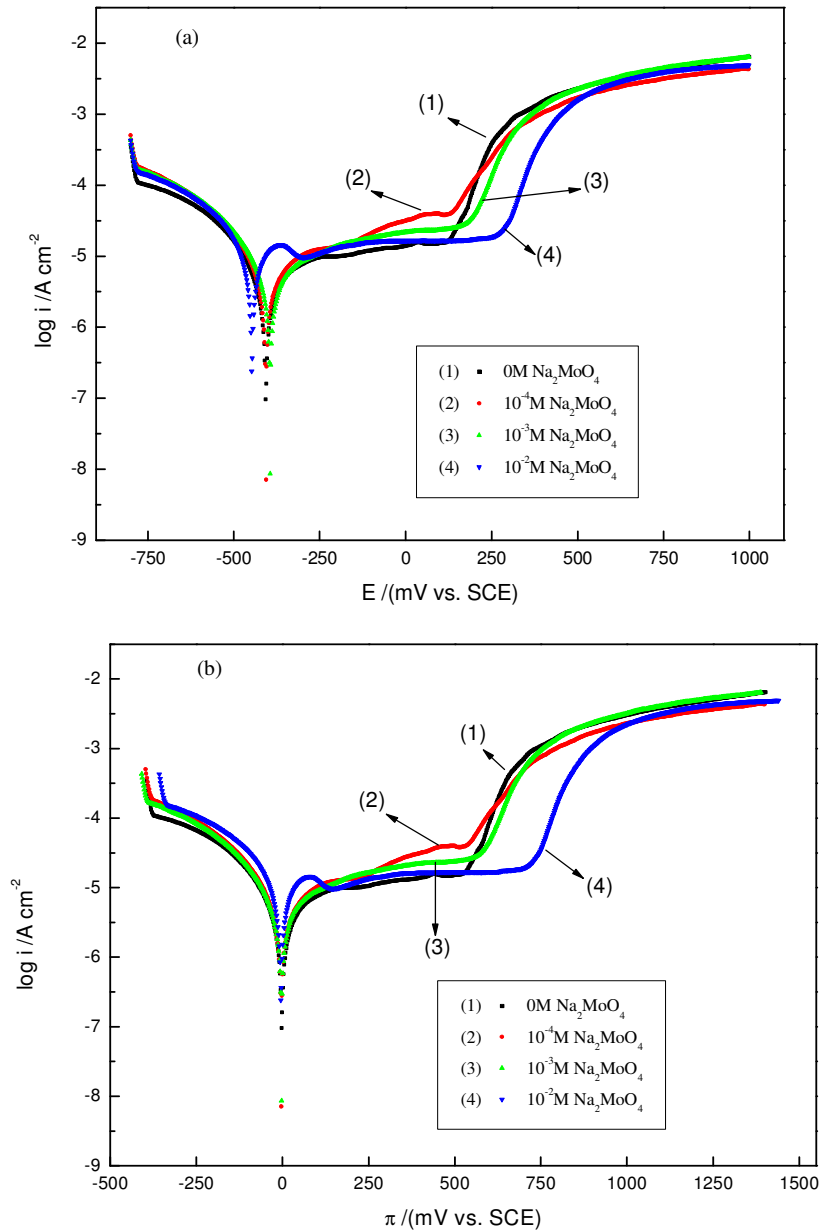


**Figure 8.** Potentiodynamic polarisation curves of pure cobalt in non deaerated solution of  $10^{-3}$  M  $\text{NaHCO}_3$  and  $10^{-3}$  M  $\text{Na}_2\text{SO}_4$  in absence and in presence of sodium molybdate, at 25 °C. (a)  $\log i = f(E)$ , (b)  $\log i = f(\pi)$ .

In absence and presence of  $10^{-4}$  M and  $10^{-3}$  M of sodium molybdate, the anodic curves have the same shape: a stable passivation plateau settles up to 0.100 V/SCE; beyond this potential, an anodic wave, probably due to an electrochemical reaction in solid phase, is observed; it would correspond to a transition to a higher oxidation degree of cobalt. In presence of  $10^{-2}$  M sodium molybdate, a passivation plateau is preceded by an active-passive peak and extends until 0.250 V/SCE.

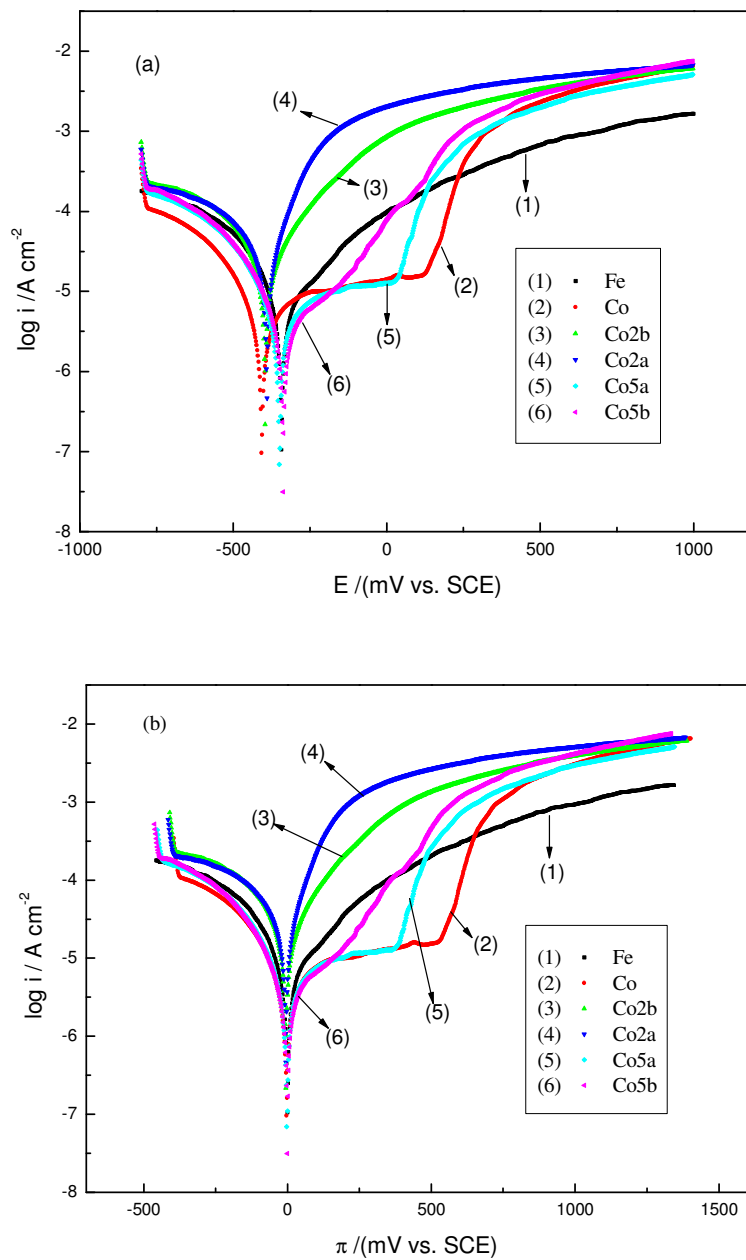


**Figure 9.** Potentiodynamic polarisation curves of iron, cobalt and the FeCoC ternary alloys in non deaerated solution of  $10^{-3}$  M  $\text{NaHCO}_3$  and  $10^{-3}$  M  $\text{Na}_2\text{SO}_4$  in absence of sodium molybdate, at 25 °C. (a)  $\log i = f(E)$ , (b)  $\log i = f(\pi)$ .

### Comparative discussion of FeCoC ternary alloys in absence of sodium molybdate

In absence of sodium molybdate, the corrosion rate of Co2a and Co2b ternary alloys containing the most important carbon content and the least important cobalt content is higher than that of iron and cobalt; their corrosion potentials lie between those of iron and cobalt. The mechanism of dissolved oxygen reduction is the same on the four samples, but with a faster kinetic on Co2a and Co2b.

The corrosion potentials of Co5a and Co5b, with the least important carbon content and the most important cobalt content, tend towards that of iron. Co5a anodic curve shows a beginning of passivation which is immediately prevented by two electrochemical reactions in solid phase. These reactions could be those of iron and cobalt to higher oxidation states. The electrochemical behaviour of Co5a is comparable with that of cobalt, with however a slightly less extensive passivation plateau and more positive corrosion potential. The rates of dioxygen cathodic reduction on Co5a and Co5b are comparable with that on cobalt. In contact of a non deaerated solution of  $10^{-3}$  M  $\text{NaHCO}_3$  +  $10^{-3}$  M  $\text{Na}_2\text{SO}_4$ , the Co5a ternary alloy of composition of 10 wt.% Co, 0.5 wt.% C is nobler than that of cobalt and more passive than that of iron, at 25 °C.

Fig. 9 shows that the anodic curves of cobalt and the four FeCoC ternary alloys tend towards the same limit of current, higher than that of iron, attesting thus that cobalt and iron are electrochemically oxidized in solid phase.

### **Comparative discussion of FeCoC ternary alloys in presence of $10^{-2}$ M of sodium molybdate**

The addition of  $10^{-2}$  M of sodium molybdate to the corrosive medium,  $10^{-3}$  M  $\text{NaHCO}_3$  +  $10^{-3}$  M  $\text{Na}_2\text{SO}_4$ , changes completely the kinetic of the ternary alloys corrosion. In fact,

- Co2a and Co2b have corrosion potentials more anodic than that of iron (table 2) and their corrosion resistance improves while passing from a more active state than that of iron (in absence of molybdate) to a quasi-passive state with a more passifying film than that of cobalt (in presence of  $10^{-2}$  M of sodium molybdate, Fig. 7 and 8);
- Co5a passivation is reinforced while extending on more large potential interval than that of cobalt;
- Co5b behaviour passes from an active dissolution to a passive dissolution.

Fig. 10 reveals that the passivation of FeCoC ternary alloys of cobalt content lower than 10 wt.% is more sensible to their cobalt content than that of their carbon content. In fact, for the two carbon compositions ( $\sim 4\%$  ;  $\sim 0.5\%$ ), the important cobalt content renders the corrosion potentials slightly more anodic than those of iron or cobalt and the film more passive than that of cobalt.

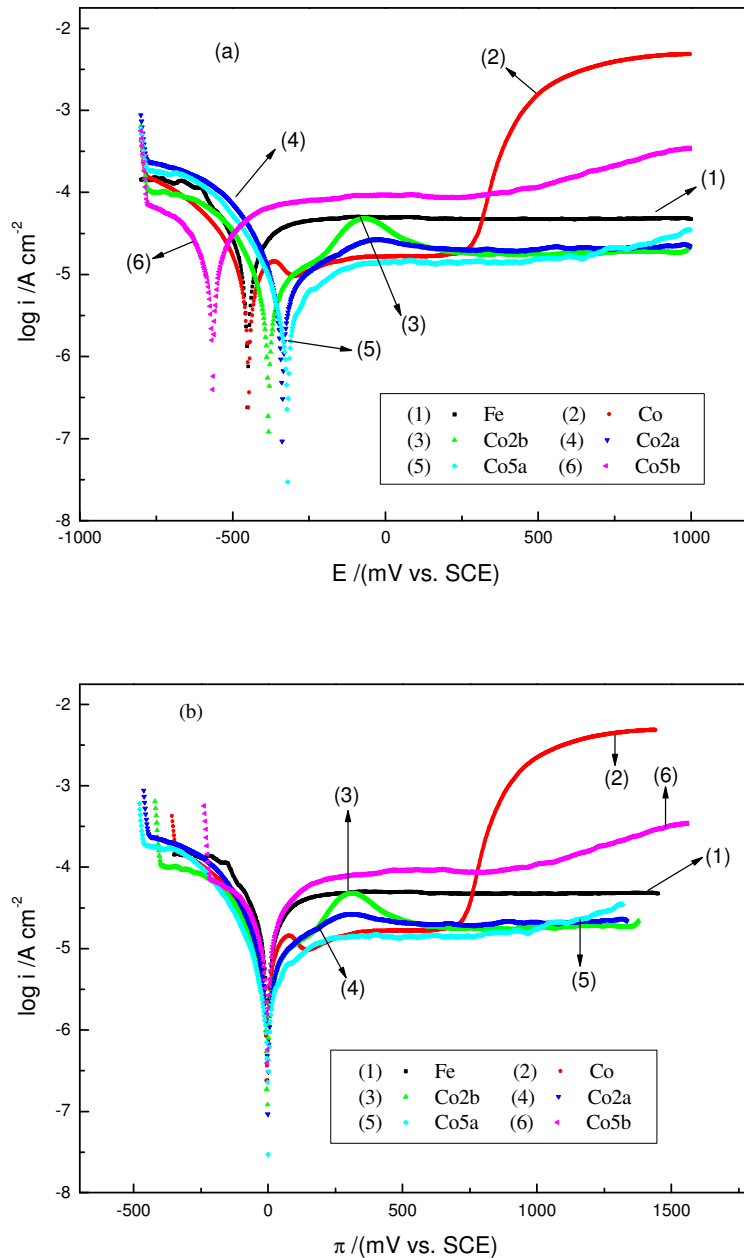


**Figure 10.** Potentiodynamic polarisation curves of iron, cobalt and the FeCoC ternary alloys in non deaerated solution of  $10^{-3}$  M  $\text{NaHCO}_3$  and  $10^{-3}$  M  $\text{Na}_2\text{SO}_4$  in presence of  $10^{-2}$  M in sodium molybdate, at 25 °C. (a)  $\log i = f(E)$ , (b)  $\log i = f(\pi)$ .

Moreover, the active-passive transition observed on Co2b and Co2a diminishes then disappears leading therefore to a quasi-passive state when the cobalt content increases in the range 4.84 – 7.25 wt.%. These observations correspond to the ratio  $(\text{wt.\%Co}/\text{wt.\%Fe}) < 0.08$ . However,  $(\text{wt.\%Co}/\text{wt.\%Fe}) > 0.08$  seems to be harmful to the FeCoC ternary alloys since for Co5b, the ternary with the most important cobalt content,

- corrosion potential shifts cathodically of more than 0.240 V, compared to that of Co5a;
- passivation plateau rises horizontally of almost 1 decade of current. The film becomes thus less passivating than that of iron and is stretched slightly to the top, from a potential which would correspond to an electrochemical oxidation reaction of cobalt, in solid phase.

## **Conclusion**

This study was interested in the synergic effect of cobalt as an alloying element and sodium molybdate as a passivating agent of FeCoC ternary alloys, in contact with a corrosive medium constituted of  $10^{-3}$  M NaHCO<sub>3</sub> +  $10^{-3}$  M Na<sub>2</sub>SO<sub>4</sub>. The results presented above allow concluding that:

- in absence of sodium molybdate, cobalt, as alloying element confers to the Co5a ternary alloy passivity almost identical to that of pure cobalt (longer passivation plateau, slightly lower passive current density and disappearance of the active-passive peak), a corrosion potential very close to that of iron and a corrosion current density lower than that of iron and even than that of cobalt;
- sodium molybdate at a concentration of  $10^{-2}$  M passivates pure iron on potential interval of more than 1.4 V, but displaces the corrosion potential of more than 0.100 V in the direction of the more negative values and multiplies approximately the corrosion current density by four;
- the effect is particularly observed for Co2a, Co2b and Co5a alloys, in presence of especially  $10^{-2}$  M sodium molybdate. In fact, these three alloys are characterised by:
  - passivation plateau extending on a more extensive potentials interval than that of pure cobalt;
  - a better passive state than that of iron;
  - nobler corrosion potentials;
  - and corrosion current densities three to four times smaller than that of pure iron, in presence of  $10^{-2}$  M MoO<sub>4</sub><sup>2-</sup>;
- for the ratio (wt.%Co/wt.%Fe)<0.08, the film becomes more passif than that of cobalt while the ratio (wt.%Co/wt.%Fe)>0.08 seems to be harmful to the FeCoC ternary alloys, since for Co5b, with the most important cobalt content, the film is less passivating than that of iron;
- in addition, this study showed that molybdate ions being thermodynamically non reducible, in the conditions of this work, the increase of current density with anodic displacement of corrosion potential can be interpreted by a kinetic character of reduction process of dioxygen on iron electrode, in presence of molybdate ions. An application to the dosage of the molybdate ions is to be considered in these conditions.

## References

1. A. Weisstuch and C.E. Schell, *Corrosion-Nace* Vol. 28, N° 8 (August 1972) 299-306.
2. D.R. Robitaille, *Materials Performance* 15 (1976) 40-44.
3. M. Saremi, C. Dehghanian, M. Mohammadi Sabet, *Corrosion Science* 48 (2006) 1404-1412.
4. D.R. Robitaille, *Industrial Water Engineering* (November/December 1979) 14-19.
5. G.H. Cartledge, *Corrosion-Nace* Vol. 24, N° 8 (August 1968) 223-236.
6. M.S. Vukasovich and D.R. Robitaille, *Journal of the Less-Common Metals* 54 (1977) 437-448.
7. M.A. Stranick, *Corrosion-Nace* Vol. 40, N° 6 (June 1984) 296-302.
8. I.J. Yang, Proceedings of the 7<sup>th</sup> European Symposium on Corrosion Inhibitors (7SEIC), Ann. Univ. Ferrara, N. S., Sez. V, Suppl. N. 9 (1990) 919-930.
9. D.G. Kolman and S.R. Taylor, *Corrosion* 49, N° 8 (August 1993) 635-643.
10. J.M. Zhao, Y. Zuo, *Corrosion Science* 44 (2002) 2119-2130.
11. G.O. Ilevbare, G.T. Burstein, *Corrosion Science* 45 (2003) 1545-1569.
12. C.R. Alentejano, I.V. Aoki, *Electrochimica Acta* 49 (2004) 2779-2785.
13. G. Mu, X. Li, Q. Qu, J. Zhou, *Corrosion Science* 48 (2006) 445-459.
14. K. Aramaki, *Corrosion Science* 43 (2001) 591-604.
15. K.C. Emregül, A.A. Aksüt, *Corrosion Science* 49 (2003) 2415-2433.
16. E.E. Ait Addi, L. Bazzi, M. Elhilali, R. Salghi, B. Hammouti, M. Mihit, *Applied Surface Science* 253 (2006) 555-560.
17. K.-H. Na, S.-I. Pyun, *Journal of Electroanalytical Chemistry* 596 (2006) 7-12.
18. M.S. Vukasovich and G.G. Van Riper, Proceedings of the 7<sup>th</sup> European Symposium on Corrosion Inhibitors (7SEIC), Ann. Univ. Ferrara, N. S., Sez. V, Suppl. N. 9 (1990) 673-683.
19. C.M. Mustafa, S.M. Shahinoor Islam Dulal, *Corrosion* 52 N° 1 (1996) 16-22.
20. A.M. Shams El Din, L. Wang, *Desalination* 107 (1996) 29-43.
21. M. Meziane, F. Kermiche, C. Fiaud, *British Corrosion Journal* 33 N° 4 (1998) 302-308.
22. D.R. Lide, Handbook of Chemistry and Physics, 78<sup>th</sup> Edition, 1997-1998.
23. Valéria A. Alves, Christopher M.A. Brett, *Electrochimica Acta* 47 (2002) 2081-2091.
24. T. Kodama, R. Ambrose, *Corrosion-Nace* Vol. 33 N°5 (1977) 155-161.
25. A.J. Bentley, L.G. Earwaker, J.P.G. Farr, M. Saremi, A.M. Seeey, *Polyhedron* 5 N° 1/2 (1986) 547-550.
26. M. Ürgen, A.F. Cakir, *Corrosion Science* 32 N° 8 (1991) 841-852.
27. S. Virtanen, B. Surber, P. Nylund, *Corrosion Science* 43 (2001) 1165-1177.